J Mol Model (2013) 19:4283–4291
DOI 10.1007/s00894-013-1939-0

ORIGINAL PAPER

Theoretical design of donor-acceptor conjugated copolymers based on furo-, thieno-, and selenopheno[3,4-c] thiophene-4,6-dione and benzodithiophene units for organic solar cells

Xiaorui Liu · Rongxing He · Wei Shen · Ming Li

Received: 9 May 2013 / Accepted: 8 July 2013 / Published online: 31 July 2013

Abstract In this work, a series of donor-acceptor (D-A) copolymers (PBDTFPD(Pa1), PBDTTPD (Pa2) and PBDTSePD(Pa3)) were selected and theoretically investigated using O3LYP/6-31G(d), PBE0/6-31G(d), TD-O3LYP/6-31G(d)//O3LYP/6-31G(d) and periodic boundary conditions methods. The calculated results go well with the available experimental data of highest occupied and lowest unoccupied molecular orbital (HOMO/LUMO) energy levels and band gaps. A series of conjugated polymers (Pb1~Pb3) comprised of electron-deficient benzodithiophene and electron-rich furo-, thieno-, and selenopheno[3,4-c]thiophene-4,6-dione were further designed and studied. Compared with Pa1-Pa3, the designed polymers of Pb1~Pb3 show better performances with smaller band gaps, lower HOMO energy levels, red shift of absorption spectra, and larger open circuit voltage (Voc). For investigated polymers (Pa1, Pa2, Pa3, Pb1, Pb2, Pb3), the power conversion efficiencies (PCEs) of ~6.1 %, ~7.2 %, ~7.9 %, ~8.0 %, ~9.5 % and ~9.0 % are predicted by Scharber diagrams when they are used in combination with PC60BM as an acceptor. The results illustrate that these designed polymers which turn the electron-withdrawing capability in D-A conjugated polymers are expected to turn into highly efficient donor materials for organic solar cells.

Keywords Benzodithiophene · Density functional theory · Hole mobility · Optical absorption · Organic solar cell · Power conversion efficiency

Electronic supplementary material The online version of this article (doi:10.1007/s00894-013-1939-0) contains supplementary material, which is available to authorized users.

X. Liu · R. He · W. Shen · M. Li (✉)
School of Chemistry and Chemical Engineering,
Southwest University, Chongqing 400715, China
e-mail: liming@swu.edu.cn

Introduction

Organic solar cells based on conjugated polymers have attracted great attention in recent years as they enjoy a lot of advantages, such as low cost, light weight, and large-area processabilty [1–7]. There is a key component in organic solar cell, active layer, which blends an electron donor polymer and an electron acceptor placed between a tin-doped indium oxide (ITO) anode and an Al cathode [8, 9]. Fullerene and its derivates are usually used as acceptor materials (for example: 6,6-phenyl-C61-butyric acid methyl ester or [6,6]-phenyl C71 butyric acid methyl ester (PC60BM or PC70BM)) [10–14]. The performance of polymer solar cell was increased dramatically in the past few years. For instance, the power conversion efficiency (PCE) of ~9 % was achieved by using low band gap of donor-acceptor (D-A) polymer in the bulk-heterojunction (BHJ) structure solar cells [15].

The PCE of organic solar cell device is proportional to the open circuit voltage (Voc), the short-circuit current (Jsc) and the fill factor (FF). The Jsc depends on the efficiencies of the light absorption of the active layer, exciton diffusion and dissociation at the donor/acceptor interface, charge transport in the active layer, and charge collection on the electrodes [16–18]. Voc is mainly proportional to the energy level difference between the lowest unoccupied molecular orbital (LUMO) of the acceptor and the highest occupied molecular orbital (HOMO) of the donor [19]. FF is related to the series and parallel resistances of the devices, lower series resistance and higher parallel resistance result in higher FF values [16]. Therefore, the main strategies to improve the efficiency of organic solar cells include the following requirements: [16, 20–23] one is reducing the HOMO energy of the donor polymer to increase the Voc. Another is decreasing the HOMO-LUMO gap of a polymer to obtain more sunlight, which leads to a higher Jsc. Moreover, the difference between

LUMO energies of donor and acceptor should be about 0.3 eV to ensure effective electron transfer at the donor/acceptor interface. The last is that donor or acceptor should be provided with high charge carrier mobility to enhance the charge transport efficiency (to increase Jsc) and to increase FF of the devices. Definitely, in the fabrication process of the BHJ solar cell (BHJSC) device, the solubility and morphology of photovoltaic material also influence the efficiency of organic solar cell device significantly [17].

To improve efficiency of the organic solar cell device, it cannot be separated from the development of new materials. Quantum chemistry, especially molecular modeling techniques play an important role in reducing the cost of new materials development and shortening the development period of the material. In experiment, the band gaps (E_g) and HOMO energy levels are obtained by cyclic voltammetry (CV) or ultraviolet photoelectron spectroscopy (UPS) [2, 24]. The LUMO energy level is subsequently estimated by the equation, LUMO=HOMO+E_g [2, 24–26]. Quantum chemical methods have been widely used to explain and predict orbital energy levels and band gaps of molecules, especially for unknown conjugated polymers [12, 27–33]. For instance, Ku and co-workers [28] have revealed that the calculations by DFT combined with TDDFT at B3LYP/6-311G(d,p) with a dimer model can reproduce the experimental HOMO/LUMO levels and the band gaps of push-pull type copolymers. Zhang and Pei et al. [33] showed that the most accurate HOMO energy level of a polymer was predicted by PBE0/6-311G** method with a monomer model. In addition, the periodic boundary conditions (PBC) approach also was found to be a very good method to predict the HOMO and band gap of conjugated polymers reliably [30, 32, 34]. Shuai and co-works [35] studied the effect of the charge carrier mobility on the PCE of polymer solar cells theoretically. They concluded that there is a positive correlation between the PCE of polymer solar cells and the charge carrier mobility of donors to some extent. From those works performed by predecessors, they provided some important information to design and judge a highly efficient copolymer donor of organic solar cell.

Thieno[3,4-c]pyrrole-4,6-dione(TPD) is one of the most electron-deficient units to construct a low band gap conjugated donor polymer due to its strong electron-withdrawing capability [36–40]. Beaupré and co-works [41] reported the synthesis of new furo[3,4-c]pyrrole-4,6-dione (FPD) and selenopheno[3,4-c]pyrrole-4,6-dione (SePD) derivatives where the sulfur atom in the heterocycle of TPD has been replaced respectively by an oxygen or a selenium atom. Recently, D–A copolymers based on the electron-deficient unit (TPD) and electron-rich benzodithiophene(BDT) have drawn considerable attention in the literature [42–46], and the PCE of corresponding solar cell devices have approached ~7.1 % [47].

In this work, three D-A copolymers (PBDTFPD(Pa1), PBDTTPD (Pa2) and PBDTSePD(Pa3)) which contains the electron-rich BDT and three electron-deficient units (FPD, TPD and SePD), were calculated on the HOMO energy levels and the band gaps by a theoretical quantum-chemical method. Based on those calculated results, we hence replaced electron-deficient units with furo[3,4-c] thiophene-4,6-dione (FTD), thieno[3,4-c] thiophene-4,6-dione (TTD), and selenopheno[3,4-c] thiophene-4,6-dione(SeTD) in Pa1, Pa2 and Pa3 respectively, and have designed three new D-A copolymers. These designed polymers (as shown in Fig. 1) of PBDTFTD(Pb1), PBDTTTD(Pb2) and PBDTSeTD(Pb3) were theoretically investigated using the same methods on the structures, orbital energy levels, band gaps and optical spectra. In addition, we investigated the transport properties of all polymers and further estimated the performance of all designed polymer corresponding solar cell devices. Our purpose is to provide structural guidelines for selecting the suitable electron-withdrawing group and optimizing geometry of copolymer donors to further improve performance of donors in BHJSCs applications.

Computational methods

In the present work, the geometry optimization of the copolymers (dimer models) in the ground state were fully optimized employing density functional theory (DFT) with O3LYP, [48] B3LYP and PBE0 [49] functional at the 6-31G(d) basis set levels [50–52]. Three famous methods O3LYP, B3LYP and PBE0 include 11.6 %, 20 %, and 25 % Hatree–Fock (HF) exchange, respectively. There are no imaginary frequencies at this level for all the structures of optimization, which indicate that all the optimized structures are the global minima on the potential energy surface and stable structures. In the calculations, the side chain alkyl of copolymers was repacked by hydrogen atom, because they merely aided in improving solubility without affecting electronic properties [12, 53]. The polymers were calculated by

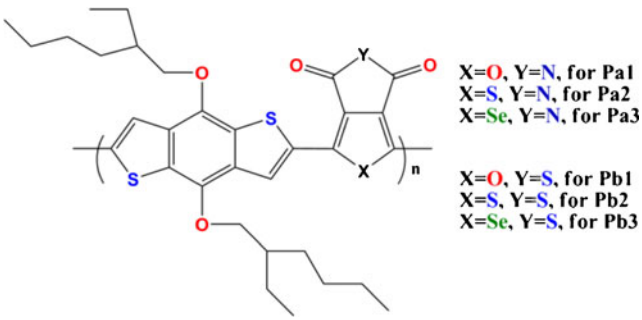

Fig. 1 The chemical structure of donor-acceptor copolymers, the Pb1~Pb3 stand for designed copolymers

periodic boundary conditions (PBC) method [32]. The HOMO and Eg of polymers were calculated by PBC-PBE0, PBC-O3LYP and PBC-B3LYP methods. PBC-PBE0 calculations were also performed using the 6-311G(d,p) basis set for Pa1-Pa3. The tested and compared results indicate that, for the polymers of Pa1-Pa3, the HOMO energy and band gap are positively associated with the percentage of the HF exchange in the functional, and that the PBE0 (for HOMO) and O3LYP (for band gap) give a smaller deviation from the experiment values than the other functional. The electron densities of all orbitals that related to the electron transitions were visualized with Multwfn 2.1 [54]. The electronic absorption spectra of dimer models for Pa1 were calculated by time-dependent density functional theory (TD-DFT) at O3LYP, B3LYP and PBE0 functional at the 6-31G(d) basis set levels in gap. Compared with the experimental data, the O3LYP obtained the more accurate vertical excitation energy. Moreover, the vertical excitation energy of dimer for Pa1 was calculated by O3LYP with different basis sets (6-31G(d,p), 6-31G(d,p) and 6-311G(d,p)) in order to inspect the influence of basis sets on calculating results. In the computation of the reorganization energy, the cation geometry of molecules were also carried out at levels of DFT/PBE0/6-311G(d,p), and the energy of the neutral geometry based on the optimized cation geometry, was obtained from single point energy computation in the same method [23, 55, 56]. The correlative computations of transfer integral are performed at the DFT/pw91pw91/6-31G(d,p) level on monomers [57]. All DFT and TD-DFT calculations are implemented by using the Gaussian 09 software [58].

Results and discussion

The frontier orbital energy level and band gaps

The frontier molecular orbital energies and Eg values have close relation with the solar-cell efficiencies [19, 28]. Therefore, it is critically important to verify our calculation method at first on the basis of providing experimental measurements on these properties. In the work, for the polymers, the calculated results of the HOMO energy levels at PBC-PBE0/6-31G(d) level (−5.56 eV, −5.51 eV and −5.49 eV for Pa1, Pa2 and Pa3, respectively) go well with the experimental values of polymers (−5.65 eV, [41] −5.56 eV [41] and −5.51 eV [41] for Pa1, Pa2 and Pa3, respectively). Moreover, we chose two types of hybrid functionals including O3LYP and B3LYP at 6-31G(d) on Pa1. In Table 1S, the calculated results of HOMO energy levels by other functionals obviously deviate from the experimental data. Moreover, the HOMOs of Pa1-Pa3 using PBC-PBE0/6-311G(d,p) methods are −5.73 eV, −5.67 eV and −5.66 eV. With the same method at 6-311G(d,p) basis set levels, the HOMOs of polymers (Pa1-Pa3) increased by about 0.17 eV. Interestingly, compared with the PBC-PBE0/6-31G(d) level on Egs (2.70 eV, 2.52 eV and 2.45 eV) of Pa1-Pa3, the Egs (2.69 eV, 2.52 eV and 2.43 eV) of Pa1-Pa3 have no significant difference from PBC-PBE0/6-311G(d,p) calculations. Hence, to save computational time and in agreement with the experimental values, the HOMO energy level of all polymers are calculated at PBC-PBE0/6-31G(d) level.

There are many methods to calculate the Eg of polymers, such as the periodic boundary conditions (PBC) approach and oligomer extrapolation etc. [32, 34]. In this work, the Eg of polymer was calculated and estimated by PBC-O3LYP at 6-31G(d) basic set. The calculated Egs of Pa1-Pa3 are 1.98 eV, 1.83 eV and 1.76 eV, respectively. The calculated values of Eg are in agreement with the experimental values of polymers (1.86, [41] 1.81[41] and 1.76 eV[41] for Pa1, Pa2 and Pa3, respectively). Therefore, the band gap of all polymers were calculated using PBC-O3LYP method at 6-31G(d) level.

The LUMO energy level is subsequently calculated from the equation, LUMO=HOMO+E_g [2, 24–26]. The calculated LUMO energy levels of Pa1-Pa3 are −3.58 eV, −3.68 eV and −3.73 eV, respectively. The experimental LUMO energy levels of Pa1-Pa3 are −3.79 eV[41], −3.75 eV [41] and −3.75 eV[41], respectively.

Molecular design of new polymer donors

In order to design a highly efficient material of polymer donor for organic solar cell, several models have been proposed to estimate the polymer performance in BHJSCs [19, 23, 59, 60]. Taking the effective electron transfer from the polymer to the acceptor into account, the ideal donor LUMO energy level should be higher than −4.0 eV [59]. Additionally, considering the solar emission spectrum and the open circuit potential of the resulting solar cell, the optimal band gap should range from 1.2 to 1.9 eV [59]. Therefore, the ideal polymer HOMO energy level should range from −5.2 to −5.8 eV [59]. Based on the above requirements, we designed a class of polymers in order to present Pb1~Pb3 in Fig. 1. Optimized geometry of all dimer models were presented in Fig. 1S. Geometry parameters of all dimer models were listed in Tables 2S and 3S. Our goal of this research is to adjust the electron-withdrawing capability in D-A conjugated polymers and to improve the electrical and optical properties and the efficiency of the photovoltaic device.

As shown in Table 2S (calculated at PBE0/6-31G(d)level), the lengths of carbon-carbon single bond (C-C) between the electron-rich unit and electron-withdrawing unit for Da1-Db3 are all within 1.431–1.444 Å. The dihedral angles of Da1-Da3 and Db1-Db3 are in the sequence Da3>Da2>Da1 and Db3>Db2>Db1, respectively. These molecules have similar

backbones. However, the planarity of the Da3 is the worst and Da1 is the best in the series of Da1-Da3, and a similar tendency also exists for Db1-Db3. The possible reason is that the diameter of the selenium, sulfur and oxygen atom in electron-withdrawing units is in the order selenium > sulfur > oxygen, which results in a weak steric hindrance to adjacent units in the molecules [33]. As shown in Table 3S, geometry parameters of all dimer models (calculated at O3LYP/6-31G(d)level) are similar to that of all dimers calculated by means of PBE0/6-31G(d) methods.

We calculated the HOMO energy levels of Pb1-Pb3 from the PBC-PBE0/6-31G(d) methods. The Egs of Pb1-Pb3 were calculated by PBC-O3LYP method at 6-31G(d) level. Table 1 shows that the HOMO energy levels of Pb1-Pb3 are −5.80 eV, −5.72 eV and −5.71 eV, respectively, and the Egs of those polymers are 1.93 eV, 1.80 eV and 1.82 eV, respectively. The LUMO energy levels (−3.87 eV, −3.92 eV and −3.89 eV for Pb1~Pb3, respectively) were calculated by the equation, LUMO=HOMO+E_g. Moreover, compared with the calculations of Pa1-Pa3, the HOMO energy levels of these designed polymers (Pb1-Pb3) are decreased by 0.24 eV, 0.21 eV and 0.22 eV, and Egs (except Pb3) are slightly reduced by 0.05 eV and 0.03 eV. The Eg of Pb3 is larger than that of Pa3 due to that the planarity of Pb3 is worse than that of Pa3 in the method of O3LYP at 6-31G(d) levels (see the Table 3S). Being more planar than Db3, Da3 shows a higher degree of hybridization and π-conjugation between the electron-rich unit and electron-withdrawing unit. This should be related to the significant reduction in the band gap of Da3. However, the Table 1 shows that the values of HOMO, LUMO and Eg are in the range of that of ideal polymer. The results indicate that those designed polymers have the narrow Egs and the ideal HOMO/LUMO energy levels, and may possess large Jsc and good air-stability when applied to BHJSCs.

Figure 2 shows the frontier molecular orbitals (FMOs) for all the dimers (computed at PBE0/6-31G(d) level). The FMOs of all dimer models have the analogous distribution characteristics. All HOMOs show the typical aromatic feature with electron delocalization for the whole conjugated dimers. The LUMOs are mainly centralized on electron-deficient unit.

Voc is a key parameter to the organic solar cell. Voc is in direct proportion to the difference of energy between the HOMO of the donor and the LUMO of the acceptor, and the formula is expressed as [19]

$$V_{oc} = (1/e)(|E_{HOMO}(D)|-|E_{LUMO}(A)|)-0.3\ \ V, \quad (1)$$

where e represents the elementary charge, and the value of 0.3 V is an empirical factor. Scharber and co-works [19] proposed the Eq. (1) using −4.3 eV as LUMO energy for the PC60BM. According to Eq. (1), the calculated Voc of Pa1-Pa3 are 1.01 eV, 0.98 eV and 0.96 eV, respectively. The calculated Voc of Pa2 (0.91 eV) close to the experimental data of Pa2 corresponding final device (Voc =0.96 eV [46]). As shown in Table 2, compared with the calculations of Pa1-Pa3, the Voc of these newly designed polymers (Pb1-Pb3) are increased by 0.24 eV, 0.21 eV and 0.22 eV.

In addition, Table 2 shows that the differences (LD-LA) of LUMO energy levels between these designed donors (Pb1-Pb3) and the acceptor of PCBM are larger than 0.3 eV, which ensures efficient electron transfer from the donor to the acceptor.

Table 1 Frontier molecular orbital energy levels and band gap of Pa1-Pb3

	Pa1	Pb1	Pa2	Pb2	Pa3	Pb3
HOMO/eV	−5.56	−5.80	−5.51	−5.72	−5.49	−5.71
Eg/eV	1.98	1.93	1.83	1.80	1.76	1.82
LUMO/eV	−3.58	−3.87	−3.68	−3.92	−3.73	−3.89

Absorption spectra

At first, several DFT methods were selected to calculate the vertical excitation energy of the dimer model of Pa1, the calculated results using three famous methods O3LYP, B3LYP and PBE0 at the 6-31G(d) basis set levels are 566 nm, 506 nm, 476 nm, respectively. Compared with the experimental absorption peak of Pa1 at 581 nm [41], O3LYP method gives relatively appropriate vertical excitation energy. Moreover, the vertical excitation energy of dimer for Pa1 was calculated by O3LYP with different basis sets (6-31G(d), 6-31G(d,p) and 6-311G(d,p)). The corresponding vertical excitation energies are 566 nm, 566 nm and 571 nm, respectively. There are no significant differences amongst the excitation energies of dimer models for Pa1 with the same method at different basis set levels. Consequently, to save the computational time, the electronic absorption spectra of dimer models for all polymers were calculated by TD-O3LYP/6-31G(d) methods.

The vertical singlet-singlet electronic transition energies and optical absorption spectra of all polymers (Pa1-Pa3 and Pb1-Pb3) were calculated by TD-O3LYP/6-31G(d)//O3LYP/6-31G(d) method with a dimer model. Figure 3 shows the simulated absorption spectra (considering the first 30 excited states). The calculated electronic transitions (the first, second and third excited states were taken into account in this work), oscillator strength, and main configurations of all these dimers are also listed in Table 3.

As shown in Table 3, the main transitions of all donors in the visible ranges and near-infrared ranges correspond to the transitions from HOMO to LUMO, HOMO-1 to LUMO and HOMO to LUMO+1. For the maximum absorptions (S1), in

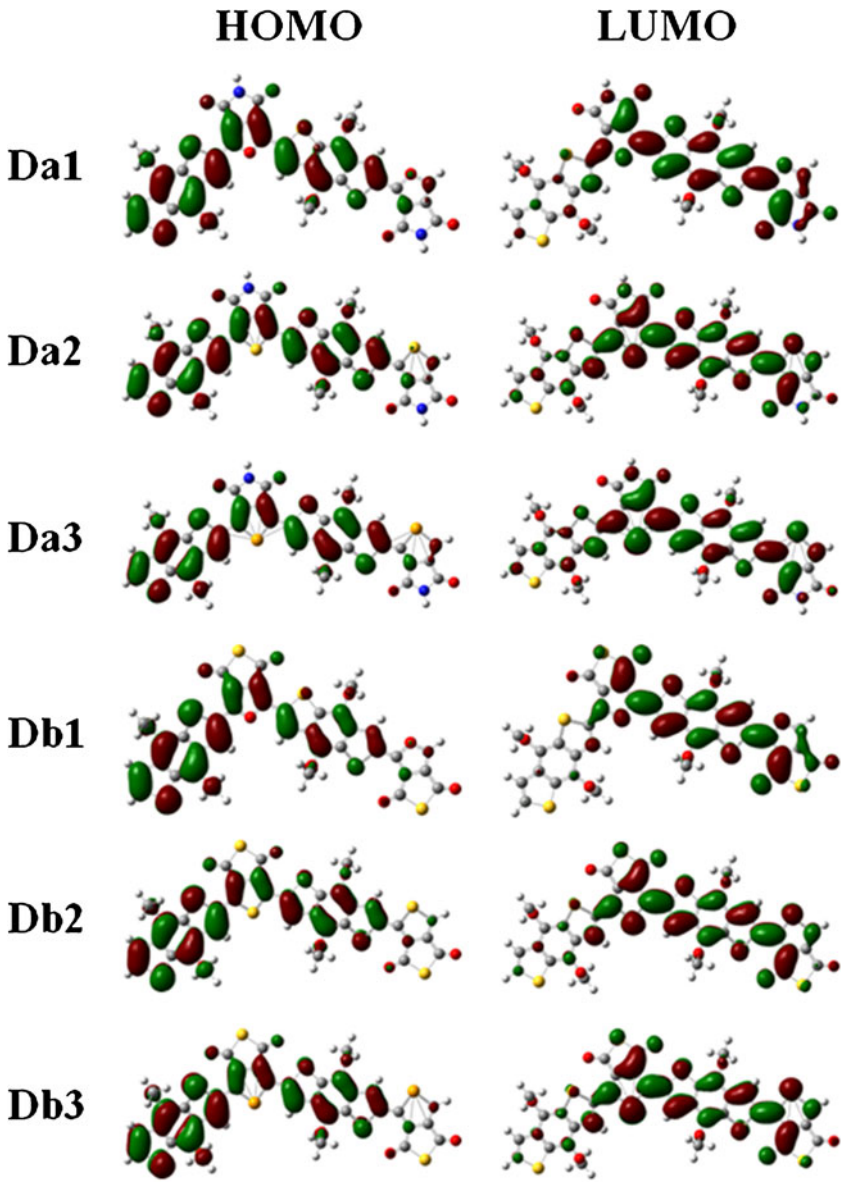

Fig. 2 Molecular orbital spatial distribution

Fig. 4 of the electron density difference plots of electron transitions, one can see that originated from HOMO→-LUMO corresponds to intramolecular electron transfer direction substantially from the electron-rich units to the electron-withdrawing units in dimer, and π→π* transitions of eletron-withdrawing units. Interestingly, a bit of electrons localized on the electron-rich unit between two electron-withdrawing units (see Fig. 4). The calculated maximum absorption peaks (Da1: 566 nm, Da2: 598 nm and Da3: 605 nm) are close to the experiments (Pa1: 581 nm, [41] Pa2: 610 nm [41] and Pa3: 635 nm [41]). We further calculated the electronic transition energies and optical absorption spectra of designed Db1-Db3 by the same method as shown in Table 3 and Fig. 3. The maximum absorption peaks for donors of Db1-Db3 are respectively about 621 nm, 647 nm and 639 nm. The calculated Eg of all dimers by O3LYP/6-31G(d) methods are 2.28 eV(Da1), 2.11 eV(Db1), 2.16 eV(Da2), 2.03 eV(Db2), 2.13 eV(Da3) and 2.06 eV(Db3). From Table 3 and Fig. 3, it can be found those red shifts occurred in the maximum absorption peaks of designed polymers, comparing with that of corresponding polymers. For instance, the maximum absorption peaks of Db1 (621 nm) are red shifted in comparison with that of Da1 (566 nm), because the Eg of Db1 is smaller than that of Da1. The results aforementioned reveal that the newly

Table 2 Open circuit voltage (Voc) and differences (L_D-L_A) of LUMO energy levels between all donors (Pa1~Pc3) and the acceptor of PC60BM

	Pa1	Pa2	Pa3	Pb1	Pb2	Pb3
L_D-L_A/eV	0.72	0.62	0.57	0.43	0.38	0.41
Voc/V	0.96	0.91	0.89	1.20	1.12	1.11
Voc(Exp.)/V		0.96[a]				

[a] from reference [46]

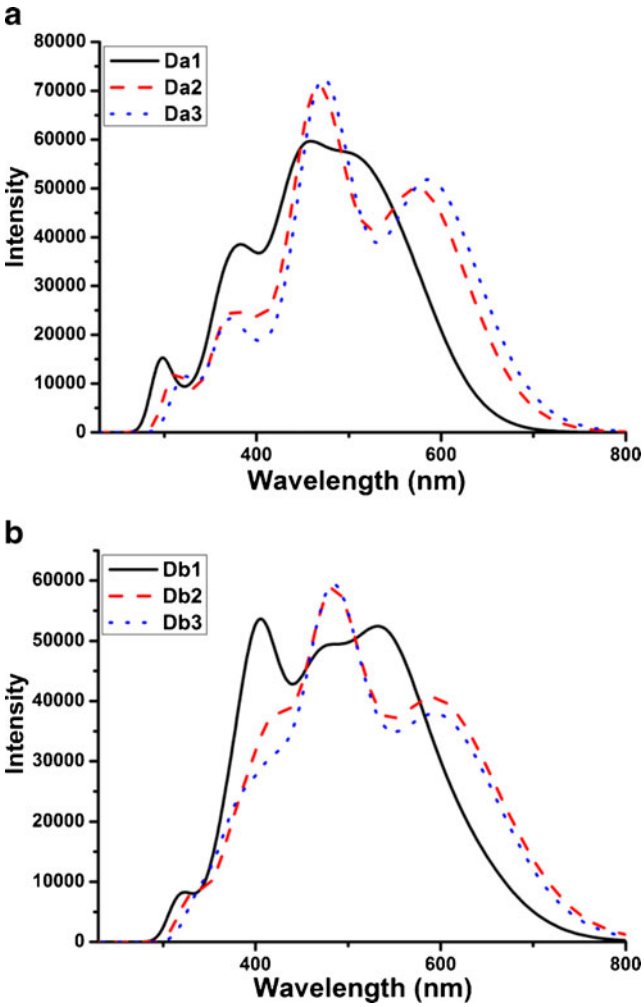

Fig. 3 The simulated absorption spectra of (**a**) Da1, Da2 and Da3; (**b**) Db1, Db2 and Db3

designed polymers have much broader absorption within the visible and infrared region, which will facilitate more efficient sunlight absorption.

Hole transport properties

In the polymer solar cell, donor as a hole transport layer with high hole mobility for the donors contributes to enhance the charge transport efficiency (to increase J_{SC} and FF) of the devices [16]. Currently, there are two types of models to describe the carrier drift in materials (the coherent band model and the hopping model) [61–63]. At very low temperature, the charge transport in materials can be described by a bandlike regime. At room temperature, it is generally accepted that the carrier transport in materials can be described as carrier hoping between neighboring molecules by the hopping model. According to Marcus-Hush theory [37, 64], the carrier transport for organic materials can be described by a hoping mechanism.

Table 3 Calculated electronic transitions, oscillator strength (f), and main configurations of all these dimers. (Assignment: H = HOMO, L = LUMO, L+1 = LUMO+1, H-1 = HOMO-1, etc.)

		Transition energy				
		E(eV)	λ(nm)	f	Major configuration	Exp. λ (nm)
Da1	S_1	2.19	566	0.33	H→L (89 %)	581[a]
	S_2	2.42	512	0.49	H-1→L (77 %)	533[a]
	S_3	2.59	479	0.17	H→L+1 (65 %)	
Da2	S_1	2.07	598	0.41	H→L (89 %)	610[a]
	S_2	2.24	554	0.36	H-1→L (84 %)	550[a]
	S_3	2.49	498	0.12	H→L+1 (81 %)	
Da3	S_1	2.05	605	0.45	H→L (89 %)	635[a]
	S_2	2.20	564	0.33	H-1→L (84 %)	565[a]
	S_3	2.48	499	0.10	H→L+1 (82 %)	
Db1	S_1	2.00	621	0.18	H→L (92 %)	
	S_2	2.26	548	0.49	H-1→L (82 %)	
	S_3	2.42	513	0.21	H→L+1 (83 %)	
Db2	S_1	1.92	647	0.22	H→L (94 %)	
	S_2	2.11	588	0.38	H-1→L (89 %)	
	S_3	2.31	537	0.14	H→L+1 (91 %)	
Db3	S_1	1.94	639	0.24	H→L (96 %)	
	S_2	2.12	584	0.33	H-1→L (91 %)	
	S_3	2.32	534	0.11	H→L+1 (92 %)	

[a] from reference [41]

The hole mobility is evaluated from the Einstein relation [65, 66],

$$\mu = \frac{eD}{K_B T}, \tag{2}$$

where e, D, K_B and T are the electron charge, the charge diffusion coefficient, Boltzmann constant and temperature, respectively. For a d-dimensional system, D is defined as the ratio between the mean-square displacement and the diffusion time:

$$D = \lim_{t\to\infty} \frac{1}{2d} \frac{\langle x(t)^2 \rangle}{t} \approx \frac{1}{2d} \sum_i r_i^2 k_i p_i \tag{3}$$

Where d is the spatial dimensionality, i runs over all nearest adjacent molecules and r_i, k_i and p_i are the corresponding center-to-center hopping distance, charge transfer rate (k), and hopping probability ($p_i = {}^{k_i}/_{\Sigma_i k_i}$), respectively. Furthermore, when considering only one neighbor, the diffusion constant along with a single molecular dimer is simply defined as: [67, 68]

$$D = \frac{1}{2} k r^2 \tag{4}$$

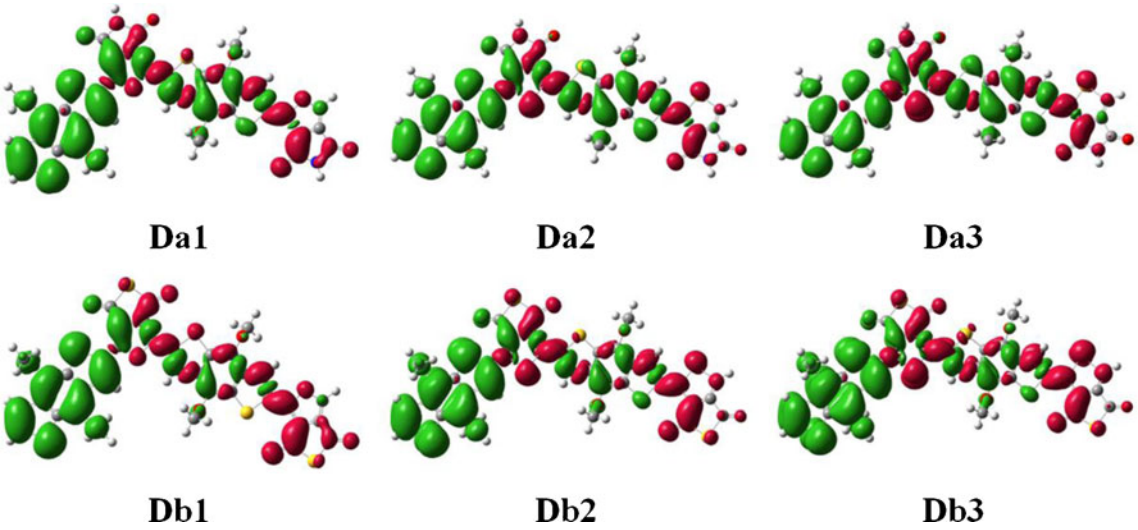

Fig. 4 Electron density difference plots of electronic transitions for all dimer models

Where k and r are the charge transfer rate and intermolecular distance for dimer, herein, the hole mobility is expressed as: [65, 66]

$$\mu = \frac{er^2}{2K_BT}k \tag{5}$$

The Marcus theory is a widely used method to estimate the carrier hoping rate: [64, 68, 69]

$$k = \left(t_h^2/h\right)\sqrt{4\pi^3/\lambda_h K_B T}\exp\left(-\lambda_h/4K_BT\right) \tag{6}$$

Where h is the Planck constant. It can be seen from Eq. (6) that there are two major parameters that determine the transport rate k, both of which are the total reorganization energy (λ) and transfer integral (t_h); the reorganization energy λ can be calculated using, [63, 68]

$$\lambda_h = \lambda_1 + \lambda_2 = (E_1 - E) + \left(E^* - E_1^*\right) \tag{7}$$

Here, λ_1 corresponds to the difference between the energies of the neutral molecule in its equilibrium geometry and in the relaxed geometry characteristic of the ion. λ_2 corresponds to the difference between the energies of the radical ion in its equilibrium geometry and in the neutral geometry. E and E_1^* are the ground-state energy of the neutral state and the energy of the charged molecular state, respectively. E_1 and E^* are the energy of the neutral molecule at the optimal ion geometry and the energy of the ion state at the optimal geometry of the neutral molecule, respectively. The transfer integral t represents the electron coupling strength of the adjacent segments and can be estimated by Koopmans' theorem [70]. The transfer integral t of hole are given by the following, [71, 72]

$$t_h = \frac{1}{2}\left(E_H - E_{H-1}\right) \tag{8}$$

where E_H and E_{H-1} are the energies of the HOMO and HOMO-1 in the closed-shell configuration of the neutral state, respectively.

The transfer integral is directly connected with the carrier hopping pathways or intermolecular stacking. It is reported that the π-stacking distance of 3.60~3.80 Å between macromolecules for Pa2 is measured by two-dimensional wide-angle X-ray scattering (2D-WAXS) [44]. In this work, we only take the face-to-face π-stacking into consideration to comparatively calculate the transport property for the monomer models extracted from corresponding polymer, and assume the π-stacking distance about 3.80 Å. The calculated transfer integral (t_h), reorganization energy (λ_h), hole mobilities (μ_h) of all systems were listed in Table 4. Table 4 shows that the hole mobility of all the monomers is in the same order of magnitude (~10^{-3} cm^2V^{-1} s^{-1}). Therefore, considering the abilities of hole transport, designed polymers have good transport properties (to increase the J_{SC} and FF) for donors in organic solar cell.

Solar cell performances

Generally, the polymer solar cells are based on the BHJ structure of the blend of conjugated polymer donors and

Table 4 Computed transfer integral, reorganization energy, hole transport rates and hole mobilities of all monomer models, all energy is eV

	t_h	λ_h	k_h/s^{-1}	μ_h/cm^2V^{-1} s^{-1}
Ma1	0.168	0.788	2.61×10^{11}	7.33×10^{-3}
Ma2	0.168	0.875	1.07×10^{11}	3.00×10^{-3}
Ma3	0.170	0.866	1.20×10^{11}	3.37×10^{-3}
Mb1	0.169	0.829	1.73×10^{11}	4.86×10^{-3}
Mb2	0.165	0.888	9.01×10^{10}	2.53×10^{-3}
Mb3	0.166	0.880	9.90×10^{10}	2.78×10^{-3}

fullerene derivative acceptors. Scharber and Mühlbacher et al. [19] have proposed a relationship between the PCE of the PC60BM-based BHJSC and the band gap and the LUMO level (or HOMO level). Recently, Ku [28] and Zhang [33] employed the Scharber model [19] to predict PCE of the solar cell made by D-A copolymer donor and PCBM. They concluded that to a certain extent with Scharber model to predict PCE of the solar cell can obtain an accurate result consistent with the experimental data. To estimate the designed polymers, we used the Scharber model to predict PCEs (%) of the solar cells combining with each polymer and PC60BM. Scharber model is based on the observation that efficient solar cell performance can be brought forward by high open-circuit voltage (Voc, which is given by the relationship Voc=−HOMO-4.6, in electron volts) and high Jsc, which is given by the integration of the solar spectrum for the photon energies equal to or larger than the band gap of the donor) as well as high fill factor (FF, which is assumed to be a constant value of 0.65) [19]. According to the Scharber model, one can make predictions about the overall PCEs from the band gaps and the LUMO energy levels of the polymer donors. The prediction (using the calculated results of Eg and LUMO energy levels) by the Scharber model shows that the predicted PCEs (~7.2 %) of Pa2 are in agreement with the experimental data (7.1 %) [47]. To our knowledge, there has been no efficiency data reported for solar cells made of Pa1 or Pa3. According to the Scharber model, the PCEs of five solar cell devices were made by Pa1, Pa3, Pb1, Pb2, Pb3 and PC60BM are ~6.1 %, ~7.9 %, ~8.0 %, ~9.5 % and ~9.0 %, respectively. It is noteworthy that other factors which were not considered in this work can give rise to significantly affect the PCE, such as the contact of the active layer with the electrodes, the morphology of the polymer/PC60BM mixture in the BHJ active layer, and so on.

Conclusions

The approach of PBE0/6-31G(d), O3LYP/6-31G(d) and TD-O3LYP/6-31G(d)//O3LYP/6-31G(d) with the dimer model have been used to study the electrical and the optical features for a series of D-A conjugated polymers. The method of PBC-PBE0/6-31G(d) and PBC-O3LYP/6-31G(d) has been taken to calculate the HOMO energy and band gap of polymers, respectively. The LUMO energy levels were calculated from the equation, LUMO=HOMO+E_g. The results indicated the methods we used in this work reproduce very well the experimental HOMO/LUMO energy levels and band gaps of Pa1-Pa3. Compared with Pa1-Pa3, the newly designed polymers of Pb1~Pb3 show better performances with smaller band gaps, lower HOMO energy levels, red shift of absorption spectra, and larger open circuit voltage (Voc). Moreover, all the polymers have good hole mobility in the ~10^{-3} cm^2V^{-1} s^{-1} magnitude. According to the Scharber models, the predicted results show that the polymers (Pa1~Pa3) and newly designed polymers (Pb1~Pb3) have high PCEs of ~6.1 %, ~7.2 %, ~7.9 %, ~8.0 %, ~9.5 % and ~9.0 %, respectively, when they are used in combination with PC60BM as an acceptor. We conclude that these polymers are good candidates for the donor materials for organic solar cell.

Acknowledgments This work was supported by National Natural Science Foundation of China (Grant No.21073144), and by Fundamental Research Funds for the Central Universities (Grant No. XDJK2010B009).

References

1. Brabec CJ, Gowrisanker S, Halls JJM, Laird D, Jia S, Williams SP (2010) Adv Mater 22:3839
2. Guo X, Zhou N, Lou SJ, Hennek JW, Ortiz RP, Butler MR, Boudreault PLT, Strzalka JW, Morin PO, Leclerc M (2012) J Am Chem Soc 134:18427
3. Fitzner R, Mena-Osteritz E, Mishra A, Schulz G, Reinold E, Weil M, Körner C, Ziehlke H, Elschner C, Leo K (2012) J Am Chem Soc 134:11064
4. Bundgaard E, Krebs FC (2007) Sol Energy Mater Sol Cells 91:954
5. Wang Z, Tao F, Xi L-y, Meng K-g, Zhang W, Li Y, Jiang Q (2011) J Mater Sci 46:4005
6. Ranjith K, Swathi S, Kumar P, Ramamurthy PC (2011) J Mater Sci 46:2259
7. Yang M, Chen X, Zou Y, Pan C, Liu B, Zhong H (2013) J Mater Sci 48:1014
8. Jeon YJ, Yun JM, Kim DY, Na SI, Kim SS (2012) Sol Energy Mater Sol Cells 105:96
9. Yi Y, Coropceanu V, Brédas JL (2009) J Am Chem Soc 131:15777
10. Sariciftci NS, Smilowitz L, Heeger AJ, Wudl F (1992) Science 258:1474
11. Guldi DM, Prato M (2000) Acc Chem Res 33:695
12. Li Y, Pullerits T, Zhao M, Sun M (2011) J Phys Chem C 115:21865
13. Imahori H, Yamada H, Guldi DM, Endo Y, Shimomura A, Kundu S, Yamada K, Okada T, Sakata Y, Fukuzumi S (2002) Angew Chem Int Ed 41:2344
14. Motaung DE, Malgas GF, Arendse CJ, Mavundla SE, Oliphant CJ, Knoesen D (2009) J Mater Sci 44:3192
15. He Z, Zhong C, Su S, Xu M, Wu H, Cao Y (2012) Nature Photonics 6:593
16. Li Y (2012) Acc Chem Res 45:723
17. Xiao S, Zhou H, You W (2008) Macromolecules 41:5688
18. Zhang Y, Zou J, Cheuh C-C, Yip H-L, Jen AK-Y (2012) Macromolecules 45:5427
19. Scharber MC, Mühlbacher D, Koppe M, Denk P, Waldauf C, Heeger AJ, Brabec CJ (2006) Adv Mater 18:789
20. Liang Y, Yu L (2010) Acc Chem Res 43:1227
21. Thompson BC, Fréchet JMJ (2008) Angew Chem Int Ed 47:58
22. Bonoldi L, Calabrese A, Pellegrino A, Perin N, Po R, Spera S, Tacca A (2011) J Mater Sci 46:3960
23. Tang S, Zhang J (2011) J Phys Chem A 115:5184
24. Seo JH, Jin Y, Brzezinski JZ, Walker B, Nguyen TQ (2009) ChemPhysChem 10:1023
25. Balan B, Vijayakumar C, Saeki A, Koizumi Y, Seki S (2012) Macromolecules 45:2709
26. Li Z, Lu J, Tse SC, Zhou J, Du X, Tao Y, Ding J (2011) J Mater Chem 21:3226

27. Xiao S, Stuart AC, Liu S, Zhou H, You W (2010) Adv Funct Mater 20:635
28. Ku J, Lansac Y, Jang YH (2011) J Phys Chem C 115:21508
29. Wang X, Sun Y, Chen S, Guo X, Zhang M, Li X, Li Y, Wang H (2012) Macromolecules 45:1208
30. Pappenfus TM, Schmidt JA, Koehn RE, Alia JD (2011) Macromolecules 44:2354
31. Zhang L, Pei K, Zhao H, Wu S, Wang Y, Gao J (2012) Chem Phys Lett 543:199
32. Zade SS, Zamoshchik N, Bendikov M (2011) Acc Chem Res 44:14
33. Zhang L, Pei K, Yu M, Huang Y, Zhao H, Zeng M, Wang Y, Gao J (2012) J Phys Chem C 116:26154
34. Zade SS, Bendikov M (2006) Org Lett 8:5243
35. Shang Y, Li Q, Meng L, Wang D, Shuai Z (2011) Theor Chem Acc 129:291
36. Hu X, Shi M, Zuo L, Nan Y, Liu Y, Fu L, Chen H (2011) Polymer 52:2559
37. Chu TY, Tsang SW, Zhou J, Verly PG, Lu J, Beaupre S, Leclerc M, Tao Y (2012) Sol Energy Mater Sol Cells 96:155
38. Zhang Y, Zou J, Yip HL, Sun Y, Davies JA, Chen KS, Acton O, Jen AKY (2011) J Mater Chem 21:3895
39. Lin Z, Bjorgaard J, Yavuz AG, Iyer A, Köse ME (2012) RSC Adv 2:642
40. Small CE, Chen S, Subbiah J, Amb CM, Tsang SW, Lai TH, Reynolds JR, So F (2012) Nature Photonics 6:115
41. Beaupré S, Pron A, Drouin SH, Najari A, Mercier LG, Robitaille A, Leclerc M (2012) Macromolecules 45:6906
42. Zou Y, Najari A, Berrouard P, Beaupré S, Réda Aïch B, Tao Y, Leclerc M (2010) J Am Chem Soc 132:5330
43. Zhang Y, Hau SK, Yip HL, Sun Y, Acton O, Jen AKY (2010) Chem Mater 22:2696
44. Piliego C, Holcombe TW, Douglas JD, Woo CH, Beaujuge PM, Fréchet JMJ (2010) J Am Chem Soc 132:7595
45. Yusoff ARBM, Kim HP, Jang J (2012) Org Electron 13:2379
46. Najari A, Beaupré S, Berrouard P, Zou Y, Pouliot JR, Lepage–Pérusse C, Leclerc M (2011) Adv Funct Mater 21:718
47. AÏch BR, Lu J, Beaupre S, Leclerc M, Tao Y (2012) Org Electron 13:1736
48. Hoe WM, Cohen AJ, Handy NC (2001) Chem Phys Lett 341:319
49. Perdew JP, Burke K, Ernzerhof M (1996) Phys Rev Lett 77:3865
50. Becke AD (1993) J Chem Phys 98:5648
51. Lee C, Yang W, Parr RG (1988) Phy Rev B 37:785
52. Cohen AJ, Mori-Sánchez P, Yang W (2012) Chem Rev 112:289
53. Tolbert LM (1992) Acc Chem Res 25:561
54. Lu T. Multiwfn 2.1 http://multiwfn.codeplex.com/
55. Lin BC, Cheng CP, Lao ZPM (2003) J Phys Chem A 107:5241
56. Lan YK, Yang CH, Yang HC (2010) Polym Int 59:16
57. Yang X, Wang L, Wang C, Long W, Shuai Z (2008) Chem Mater 20:3205
58. Frisch MJ, Trucks GW, Schlegel HB, Scuseria GE, Robb MA, Cheeseman JR, Scalmani G, Barone V, Mennucci B, Petersson GA, Nakatsuji H, Caricato M, Li X, Hratchian HP, Izmaylov AF, Bloino J, Zheng G, Sonnenberg JL, Hada M, Ehara M, Toyota K, Fukuda R, Hasegawa J, Ishida M, Nakajima T, Honda Y, Kitao O, Nakai H, Vreven T, Montgomery JA Jr, Peralta JE, Ogliaro F, Bearpark M, Heyd JJ, Brothers E, Kudin KN, Staroverov VN, Kobayashi R, Normand J, Raghavachari K, Rendell A, Burant JC, Iyengar SS, Tomasi J, Cossi M, Rega N, Millam JM, Klene M, Knox JE, Cross JB, Bakken V, Adamo C, Jaramillo JR, Gomperts RE, Stratmann O, Yazyev AJ, Austin R, Cammi C, Pomelli JW, Ochterski RL, Martin K, Morokuma VG, Zakrzewski GA, Voth P, Salvador JJ, Dannenberg S, Dapprich AD, Daniels O, Farkas JB, Foresman JV, Ortiz J, Cioslowski Fox DJ (2009) Gaussian 09, revision C.01. Gaussian, Inc, Wallingford
59. Blouin N, Michaud A, Gendron D, Wakim S, Blair E, Neagu-Plesu R, Belletête M, Durocher G, Tao Y, Leclerc M (2008) J Am Chem Soc 130:732
60. De Leeuw D, Simenon M, Brown A, Einerhand R (1997) Synth Met 87:53
61. Yang XW, Wang L, Wang C, Long W, Shuai Z (2008) Chem Mater 20:3205
62. Yang X, Li Q, Shuai Z (2007) Nanotechnology 18:424029
63. Wang C, Wang F, Yang X, Li Q, Shuai Z (2008) Org Electron 9:635
64. Marcus RA (1993) Angew Chem Int Ed 32:1111
65. Deng WQ, Goddard WA III (2004) J Phys Chem B 108:8614
66. Coropceanu V, Cornil J, da Silva D, Olivier Y, Silbey R, Bredas J (2007) Chem Rev 107:926
67. Kuo MY, Chen HY, Chao I (2007) Chem-Eur J 13:4750
68. Wang L, Nan G, Yang X, Peng Q, Li Q, Shuai Z (2010) Chem Soc Rev 39:423
69. Marcus RA (1964) Annu Rev Phys Chem 15:155
70. Koopmans T (1934) Physica 1:104
71. Liu H, Kang S, Lee JY (2011) J Phys Chem B 115:5113
72. Lan YK, Huang CI (2008) J Phys Chem B 112:14857